Application of Joint Seismic Event Location Techniques at Chuquicamata Open Pit Mine, Chile

C-I. Trifu *ESG, Canada*

V. Shumila *ESG, Canada*

I. Leslie *ESG, Canada*

Abstract

A volume of approximately 1000 x 1500 x 1000 m within the eastern wall of Chuquicamata open pit mine is monitored by a 36-channel microseismic system that includes 9 triaxial and 9 uniaxial 15 Hz omni-directional geophones. A total of 886 seismic events with moment magnitudes between -1.2 and 1.4 have been recorded and located to an average accuracy of 28 m from mid December 2006 to end March 2007. Frequency-magnitude distribution exhibits a b-value of 1.3, suggesting the failure process is characterized by a three- rather than two-dimensional behaviour within the rockmass. The largest seismic event had M_w 1.4 and occurred on February 10, 2007. Apparent stress estimates were lower than expected during an entire month leading to this event. To improve the accuracy of relative event locations, joint locations are evaluated using the collapsing and double-difference techniques. The results of the collapsing algorithm indicate that local geological structures are seismically active, with most of the seismicity occurring in two narrow bands located just inside the eastern wall, approximately parallel to its face..

1 Introduction

Despite the fact that seismic monitoring of underground mines has been employed for over 30 years, the application of this technology for the monitoring of open pit mines is relatively recent. The first successful application dates from the spring of 2002, when Cripple Creek and Victor mine operated by Anglo Gold in Colorado installed an 8-channel Hyperion system manufactured by ESG to monitor a volume of ~ 200 x 200 x 200 m during the wall retreat. The system assisted the mine personnel to quickly identify when a sill behind the wall face became seismically active and then incorporate this information into the planning of the subsequent mine development.

Located near the city of Calama, at the western edge of the Atacama Desert, more than 1200 km north of Santiago (Chile), Chuquicamata is the largest copper open pit mine in the world. Mining of this deposit began in 1915. The mine is presently operated by Codelco Norte, a division of Codelco Chile. In 2006, the mine decided to implement a seismic system in order to monitor the eastern wall. The goal was to study the general correlation between occurred seismicity, major geological features, and general mining activity, which could affect both present operations and strategic mine planning.

The scope of the present study is to document the results obtained during the seismic monitoring at Chuquicamata from mid-December 2006 until the end of March 2007. This includes a presentation of the seismic array, the analysis of event distribution and seismic source parameters, as well as the relocation of seismicity using joint relocation techniques.

2 Seismic array

Uniaxial and triaxial 15 Hz omni-directional geophones were employed for this application. The sensor array design took advantage of the presence of underground tunnels within the eastern wall, which allowed the placement of geophones at different depths. To increase the three-dimensional aperture of the seismic array three 250 m long boreholes were drilled from surface and two 200 m long boreholes were drilled on each of two underground levels. The sensor array totalled 9 triaxial and 9 uniaxial geophones and was expected to provide an event location accuracy of 30-40 m over the central monitoring volume. Figure 1 shows the type and location of these geophones in a cross section and plane view.

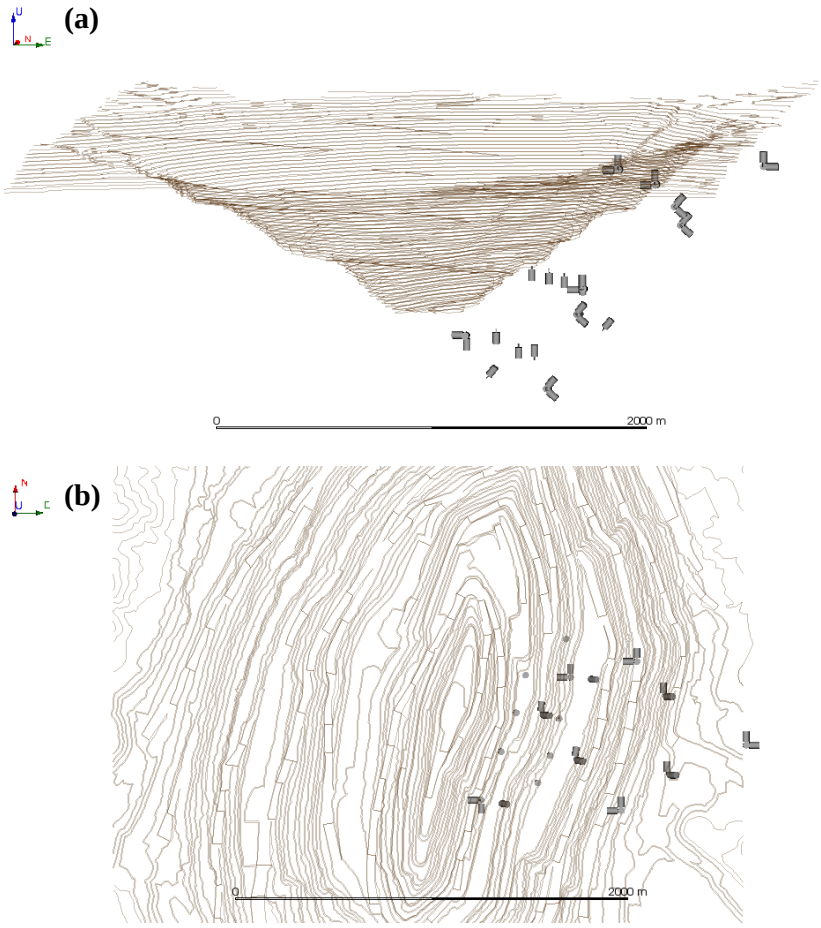

Figure 1 Seismic sensor array: (a) cross section; (b) plane view. Each sensor component is shown as a cylinder.

Seismic signals were transmitted through copper cables from geophones to the ESG's Paladin data recorders, which include pre-amplification and 24-bit resolution A/D conversion. Each Paladin is a web enabled device, with its own IP address, capable to provide continuous and/or trigger-based data acquisition. For this application, data acquisition was carried out at 5 and 20 kHz sampling for signals originating from geophones installed in boreholes drilled from surface and underground, respectively.

For the Paladins installed on surface, data communication is ensured via radio Ethernet to a unique network acquisition PC located at the portal of the underground tunnel, situated at approximately mid-depth of the open pit. Since the portal lies on the eastern wall, just below the monitoring area, radio communication required a radio Ethernet relay on the opposite wall. For the underground Paladins, Ethernet data communication to the acquisition PC was done over fibre optic cable. Time synchronization was ensured using GPS controlled time stamping with accuracy better than 1 microsecond. The acquisition and processing PC, running Microsoft Windows, was connected to the mine LAN and had Internet access, thus allowing data to be simultaneously received and processed at ESG's offices in Canada.

3 Event location and source parameters

The seismic system identified and located 1162 events that occurred between December 14, 2006 and March 31, 2007. Of these, 276 events were blasts and 886 seismic events. Example waveforms for a blast and seismic event are presented in Figures 2 and 3, respectively. Red-only seismic signals correspond to uniaxial geophones, whereas superimposed red, green and blue signals to triaxial geophones (all three components of one geophone are presented on one single trace).

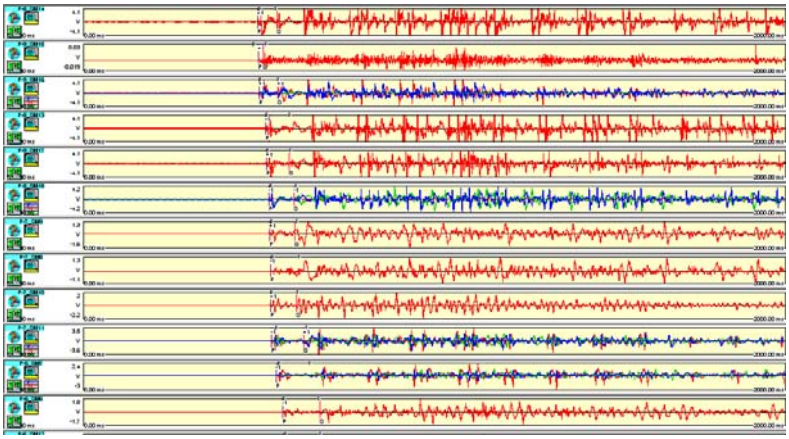

Figure 2 Example waveforms with duration of 2 s for a production blast.

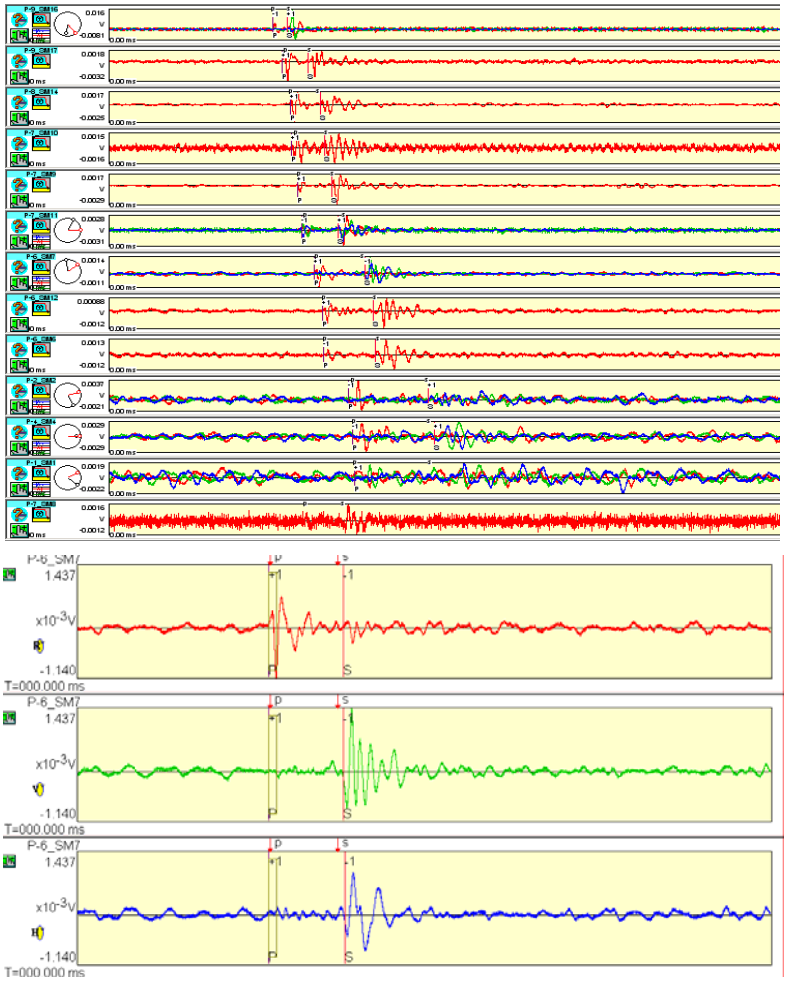

Figure 3 Example waveforms with duration of 1.3 s for a seismic event occurred January 25, 2007, at 02:43:45. Triaxial recordings are shown with different colours on the same trace (top). P, SV and SH arrivals are identified using wave polarization for trace no. 7 (bottom).

The presence of triaxial sensors in the array allows for waveform polarization analysis. This reduces the uncertainties in P- and S-wave identification and arrival time picking. Worth noting, errors in the surveying of borehole orientation and shifting effects during sensor grouting can affect the accuracy of actual sensor orientation. Thus, polarization analysis additionally allows for an independent checking of the orientations of these sensors in boreholes. Registered waveforms from blasts with known locations are employed to

calculate expected polarization of the incidence wave at each triaxial sensor. Direction cosines that define sensor's orientation are estimated from the orthogonal matrix that provides best least square fit of observed linear polarization for the radial component (P-wave) of the signal (Kabsch, 1976). The above matrix can also be obtained using the minimization of quaternion rotations (Coutsias et al., 2004). In addition to these, we also considered that optimal sensor orientation can be found under the assumption that the direction of one of the sensor axes coincides with the borehole direction, based on the so-called Rodrique's formula (Simon, 2005). The application of all three methods resulted in the retrieval of the sensor orientations to within ±3°.

Seismic events were located using mostly automatic picks, with P-wave picking based on STA/LTA (short / long term energy average) window statistics and S-wave picking employing a combination of a modified version of Cichowicz (1993) approach and energy jump criteria for uniaxial sensors. Only approximately 20% of all picks were manually reprocessed. Spatial distribution of seismic events and blasts is shown in Figure 4. Event location employed L1 norm Simplex minimization (Press et al., 1989), with the location error defined as the squared root of the sum of squared standard deviations in each spatial coordinate. Seismic events are generally located to accuracy better than 60 m, with an average location error of 28 m (Figure 5). Larger location errors for blasts are due to lack of S-wave picks.

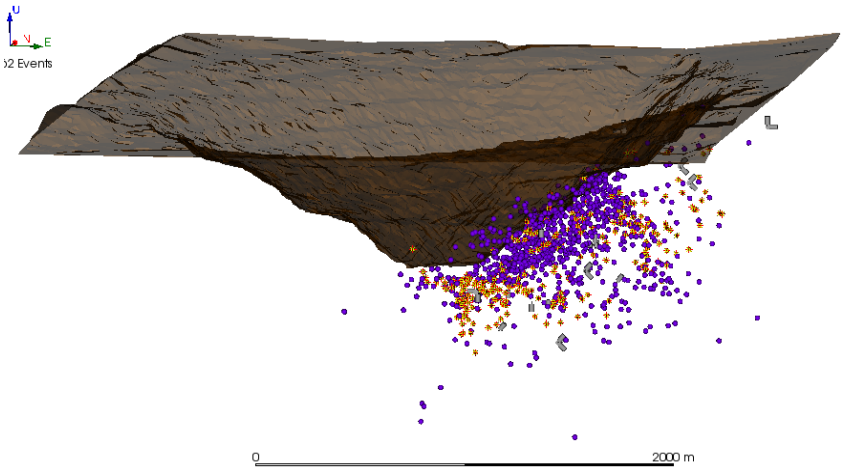

Figure 4 Distribution of seismic events (blue dots) and blasts (brown dots).

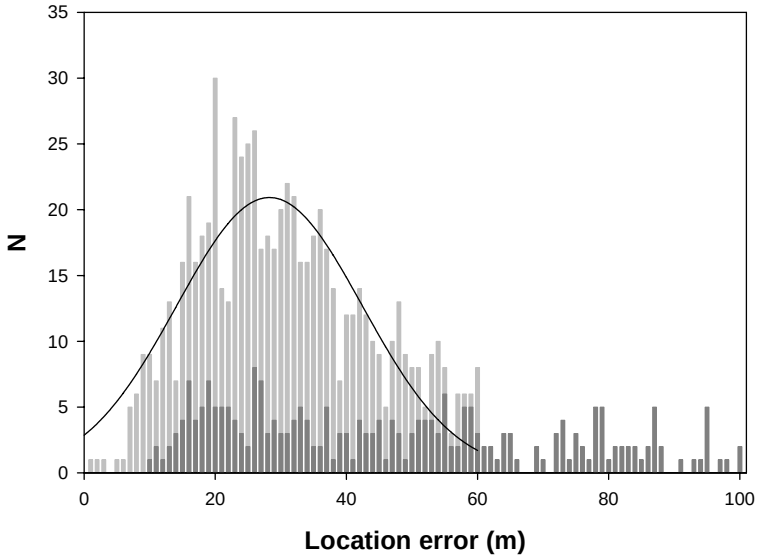

Figure 5 Event location accuracy for seismic events (light grey) and blasts (dark grey). The fit to a Gaussian distribution has a mean of 28 m and a standard deviation of 14 m.

Frequency-magnitude distribution of the seismic events outlines a b-value of 1.3 between M_w -0.7 and 1.2 (Figure 6). This indicates that the fracture process does not take place only on failure planes, but tends to spread within the monitoring volume (D = 2b or 2.6). Note how close the truncated seismic moment distribution (Kagan and Jackson, 2000) and linear regression fit the data over close to two magnitude units.

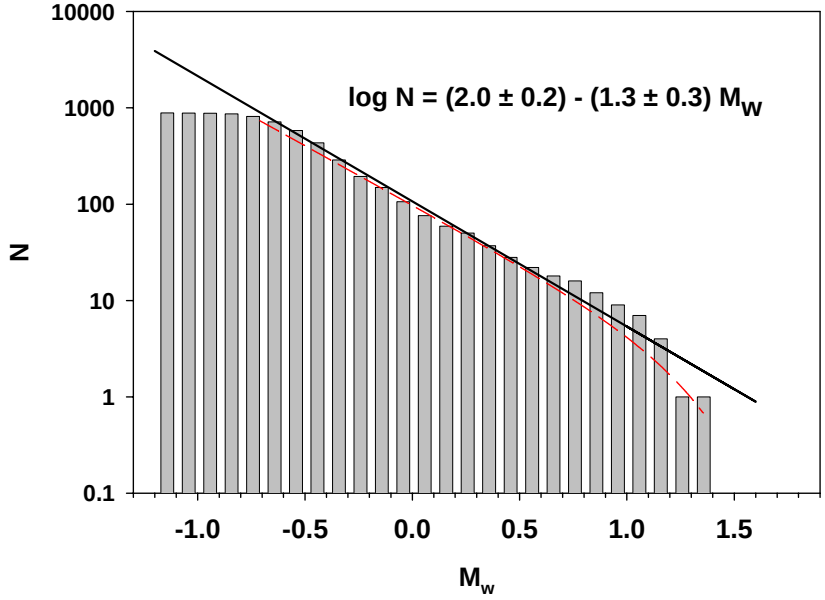

Figure 6 Cumulative frequency-magnitude distribution of the seismic events exhibits a linear trend within a wide moment magnitude range. Red curve is the truncated distribution fit.

The largest seismic event (M_w 1.4) occurred on February 10, 2007. Figure 7 shows that for about a month prior to this event the rate of cumulative seismic energy was significantly lower than that of cumulative seismic moment. Since the ratio of seismic energy to moment is proportional to apparent stress, the above result implies that during the respective period of time seismicity was dominated by events with lower apparent stress. Starting approximately January 15, a slight increase in the rate of explosives employed on site is also apparent. Note that source parameters were estimated using time integrals of squared displacement and velocity (Trifu et al, 2000) and cumulative distributions include all seismic events occurred over the monitoring time, not only those around the large event of February 10. Further detailed investigation is thus required to conclude whether the above observation is indicative of a precursory phenomenon.

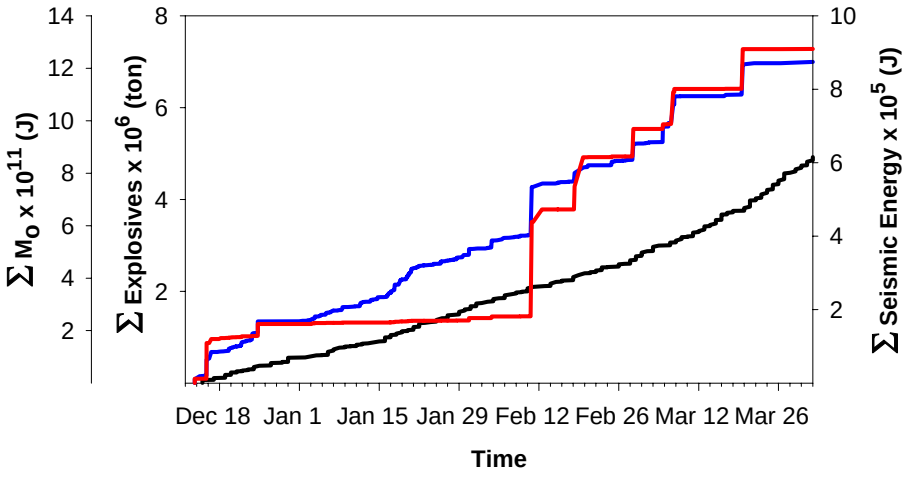

Figure 7 Cumulative seismic energy (red line), seismic moment (blue line), and amount of explosives used for both production and development blasts (black line).

4 Event relocation analysis

In order to provide a closer association of observed seismicity with pre-existing structures, two relocation algorithms were tested: collapsing and double-differences. The former technique, developed by Jones and Stewart (1997), considers that the joint location error distribution of seismic source locations whose individual location errors are normally distributed should follow a χ^2 distribution. Thus, it is possible to move each event location within its ellipsoid of uncertainty and optimize the movement of individual events to comply with the χ^2 distribution.

Figures 8 and 9 present the distribution of collapsed seismic events compared with the original event locations. Geological domains are described by Torres et al. (1997). Some clustering trends are easily apparent in the joint relocation of seismicity. Plane view and cross section representations show that most of the seismic events tend to occur in two narrow bands running just inside the wall, approximately parallel to the eastern wall face.

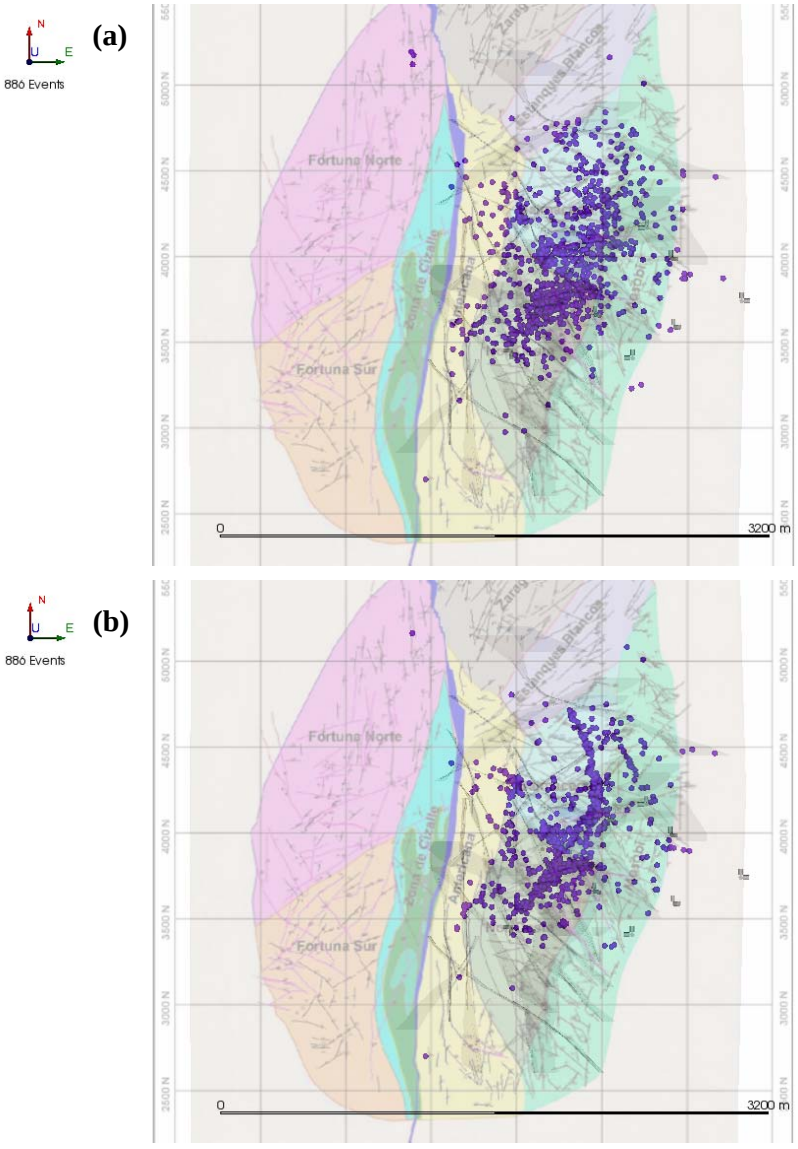

Figure 8 Plane view distribution of event locations using (a) standard absolute location and (b) relative location employing a collapsing technique.

One of these bands lies a little below the mid-depth of the pit, whereas the other band just below the pit bottom. The presence of a dense network of faults within the eastern wall renders the direct association

between occurred microseismicity and these faults a rather difficult task. However, the tight grouping exhibited by the relocated event distribution shows very good promise for subsequent analysis that may eventually outline active faulting.

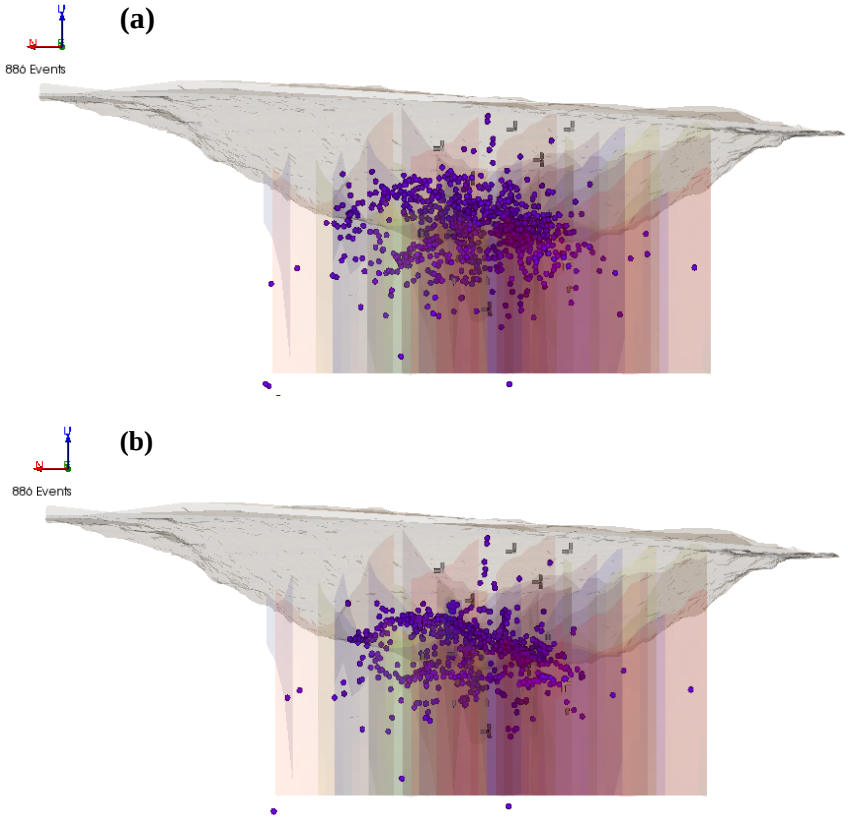

Figure 9 East trending cross section of event locations using (a) standard absolute location and (b) relative location employing a collapsing technique. Scale is similar to that in Figure 8.

The second joint relocation algorithm carries out a simultaneous minimization of residuals for pairs of sources. For events in close proximity to each other, the 'double difference' method considers that the difference in arrival times is affected only by the constant velocity to an average location (Waldhauser and Ellsworth, 2000). This allows for a system of linear equations with respect to changes in location coordinates and origin times that links the differences in arrival times at each sensor for a pair of events. Although the idea of eliminating ray path complexities and using relative information provided by combination of event-pairs in a cluster of events looks promising, the results in practice are strongly depended on data selection and weighting. A scrupulous data evaluation is required through re-weighting and filtering throughout the iterative process. Note that for a couple hundred events the system matrix for the current application has about a thousand columns and tens of thousands of rows. Solving such a system of equations requires a noticeable amount of computer time. Solution is derived iteratively, and 5-10 iterations are necessary regardless of the actual inversion methodology employed (single value decomposition or conjugate gradient).

To meet the linearity assumptions, only events located relatively far from the array were considered, for which the inter-distance between event pairs is smaller than the distance from the events to sensors. Figure 10 and 11 compare the results obtained using the double-difference algorithm with original event locations for a subset of 145 events located below the pit floor.

The results seem to indicate the presence of a slightly more elongated distribution, which tends to suggest a link between the seismicity and some underling structures. At the same time, however, the presence of some outliers is apparent.

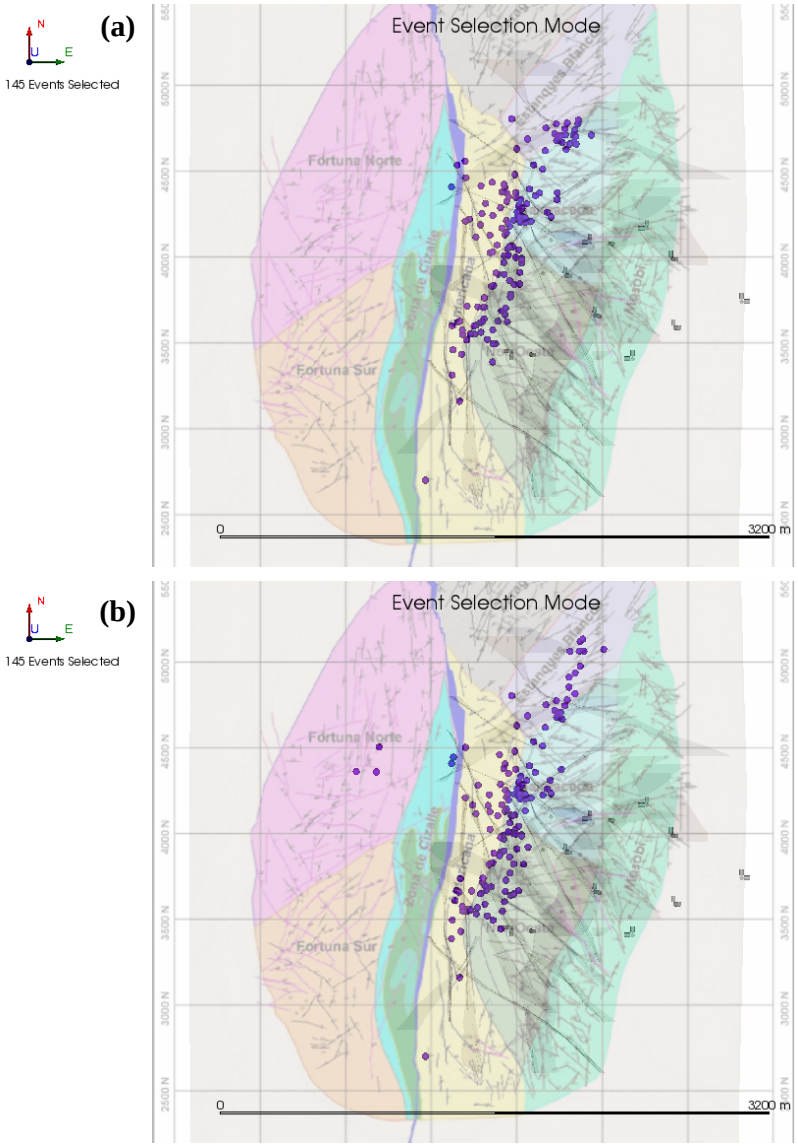

Figure 10 Plane view distribution of event locations using (a) standard absolute location and (b) relative location employing the double difference technique.

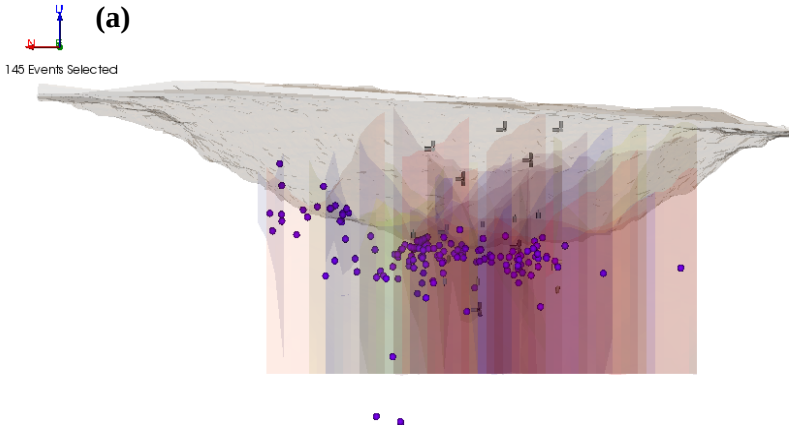

Figure 11 See caption on next page.

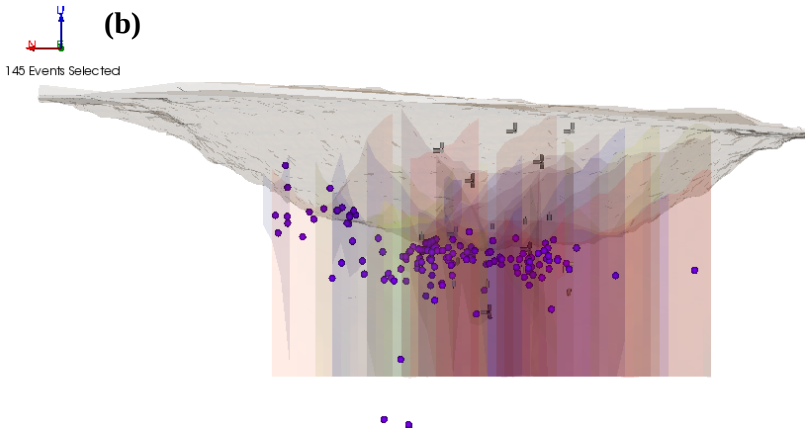

Figure 11 East trending cross section of event locations using (a) standard absolute location and (b) relative location employing the double-difference technique. Scale is similar to that in Figure 10.

5 Conclusions

A seismic array consisting of 9 triaxial and 9 uniaxial 15 Hz omni-directional geophones was installed to monitor the east wall of Chuquicamata open pit mine. Continuous 24-bit data acquisition was carried out at 5 and 20 kHz sampling frequency for the subsurface and underground geophones, respectively, employing radio and fibre optic Ethernet communication. Between December 14, 2006 and March 31, 2007, a total of 886 seismic events (M_w -1.2 to 1.4) were identified and located within average accuracy of 28 m. The slope of the frequency-magnitude distribution (b-value) is 1.3, indicating that the fracturing process tends to spread within the wall rockmass. The largest seismic event occurred on February 10, 2007 and had M_w 1.4. For a month prior to this event, seismicity was characterized by low apparent stress values, while the rate of blast explosives employed at the mine increased slightly.

Individual event locations used mostly automatic first arrival picking. To improve the relative event location accuracy, two joint event location techniques were employed: collapsing and double-differences. The former algorithm allows the events to move within their ellipsoid of uncertainty and optimize their locations to comply with a χ^2 distribution, whereas the later performs a simultaneous minimization of the differences in residuals for pairs of events close to each other. The results indicate that the collapsing technique provides a noticeably tighter distribution of seismicity, characterized by several clusters. Most of the seismic events occur in two narrow bands running just inside the eastern wall, approximately parallel to its face.

Further analysis will be focused on the use of joint event relocation results for a detailed association between the recorded seismicity, geological structures and the mining activity. Additionally, seismic moment tensor inversion will be applied to retrieve the fracture components of seismicity. This will enable the evaluation of the three-dimensional distribution of deformations and their evolution in time.

Acknowledgements

The authors would like to thank Codelco Norte for their interest and continuous support of passive seismic monitoring technology. Zenny Espinosa and Carlos Lopez from Codelco Norte, Nolberto Contador, Claudio Goich, and Patricio Toledo from EMT, Wade Coulter from ESG and Pedro Giannini from Giantec are graciously acknowledged for their contribution during the system design and installation.

References

Coutsias, E. A., C. Seok and K.A. Dill (2004) 'Using quaternions to calculate RMSD', Journal of Computational Chemistry, 25, 1849-1857.

Cichowicz, D. (1993) 'Automatic S phase picker', Bulletin of the Seismological Society of America, 83, 180-189.

Jones, R.H and R.C. Stewart (1997) 'A method for determining significant structures in a cloud of earthquakes', Journal of Geophysical Research, 102, 8245–8254.

Kabsch, W. (1976) 'A solution for the best rotation to relate two sets of vectors', Acta Crystallographica, 32, 922-923.

Kagan Y.Y. and D.D. Jackson (2000) 'Probabilistic forecasting of earthquakes', Geophysical Journal International, 143, 438-453.

Simon L.A. (2005) 'Rotations, Quaternions and Double Groups', Dover Publications.

Torres G.R., G. Flores and C. Suárez (1997) 'Caracterización Geotécnica Mina Chuquicamata', 8º Congreso Geológico Chileno, Antofagasta, 13-17 Octubre 1997, 1938-1942.

Trifu, C-I, D. Angus and V. Shumila (1997) 'A fast evaluation of the seismic moment tensor for induced seismicity', Bulletin of the Seismological Society of America, 90, 1521-1527.

Press, W.H., B.P. Flannery, S.A. Teukolsky and W.T. Vetterling (1989) 'Numerical Recipes: The Art of Scientific Computing (Fortran Version), Cambridge University Press, Cambridge, UK.

Waldhauser, F. and W.L. Ellsworth (2000) 'A double-difference earthquake location algorithm: Method and application to the northern Hayward fault', Bulletin of the Seismological Society of America, 90, 1353-1368.